Self-Energy Correction to Momentum-Density Distribution of Positron-Electron Pairs

Z. Tang,[1] Y. Nagai,[2] K. Inoue,[2] T. Toyama,[2] T. Chiba,[2] M. Saito,[3] and M. Hasegawa[1,2]

[1]*Institute for Materials Research, Tohoku University, Sendai 980-8577, Japan*

[2]*The Oarai Center, Institute for Materials Research, Tohoku University, Oarai, Ibaraki 311-1313, Japan*

[3]*Graduate School of Natural Science and Technology, Kanazawa University, Kakuma, Kanazawa 920-1192, Japan*

(Received 2 July 2004; published 16 March 2005)

Positron two-dimensional angular correlation of annihilation radiation (2D ACAR), i.e., the 2D projection of the electron momentum densities sampled by positron, in Si is employed to verify the prediction of the density functional theory within the local-density approximation (LDA). Carefully conducted test shows that the LDA introduces small but definite discrepancies to the 2D-ACAR anisotropies. Self-energy calculation using the *GW* method indicates that density-fluctuation contributes anisotropic momentum-density correction and thus improves the agreement between theory and experiment. These results provide valuable annotations to the arguments concerning the accuracy and validity of the LDA and *GW* schemes.

DOI: 10.1103/PhysRevLett.94.106402 PACS numbers: 71.15.Mb, 71.45.Gm, 78.70.Bj

Electron momentum-density (EMD) distribution represents the many-body wave function in momentum space and is a fundamental property of an interacting many-electron system. Therefore, the studies of EMD distribution provide valuable information about the nature of the many-electron interactions in solids. Density functional theory (DFT) [1] describes well the many-body interaction in the ground state of solids when the exact electron exchange-correlation potential is available. Practical computational schemes based on the DFT—using either local-density approximation (LDA) or generalized gradient approximation (GGA) to the exact exchange-correlation potential—are greatly successful in electronic-structure studies of realistic materials.

Nevertheless, recent EMD distributions in lithium obtained by Compton scattering technique exhibit significant departure from the LDA calculations [2]. Various reasons that may account for the discrepancies, such as electron correlation [3,4], thermal effect [5], etc., have been extensively discussed. Quantum Monte Carlo simulations [6,7] show that the correlation effect may *not* be the dominant source of the discrepancies; instead, the uncertainties associated with the experimental technique in probing the EMD must be invoked, because the Compton scattering accesses the EMD in an indirect way only [6]. So far, fundamentally important problems arising from the recent high-resolution EMD measurements, such as the validity and accuracy of the LDA scheme for the EMD studies and the significance of the electron correlation, are still very controversial [2–8].

This Letter addresses these controversial issues by using an alternative momentum-density technique, the positron angular correlation of annihilation radiation (ACAR). Thermalized positron in solids annihilates with an electron into (mostly) two γ photons; due to the momentum conservation, the angle of the emitted γ photons deviated from the exact antiparallelism gives directly the electron's momentum. Thus, by using a pair of position-sensitive γ-ray detectors, the positron 2D-ACAR technique measures the momentum-density distributions of the positron-sampled electrons (i.e., ACAR distribution) projected on a 2D plane [9]. We here focus on the ACAR distribution in Si, one of the best understood solids. Through carefully conducted experiments and calculations based on both the LDA and *GW* schemes, we show that there are small but definite discrepancies between the LDA calculation and experiment and that the discrepancies can be decently corrected by the self-energy effect.

The 2D-ACAR distributions in a floating-zone grown Si sample were measured at room temperature by using a state-of-the-art Anger-camera-type 2D-ACAR set recently installed in the Oarai Center, IMR, Tohoku University. The results were compared with our previous experiments done in the National Institute for Materials Science, Japan, using different facilities and sample [10], and high reproducibility of the experiments is observed (as shown later in Fig. 2).

The 2D ACAR [$N(p_x, p_y)$] is the 2D projection of the 3D momentum-density distributions of the positron-electron pairs [$\rho(\mathbf{p})$] along a chosen axis (p_z), i.e., $N(p_x, p_y) \propto \int \rho(\mathbf{p}) dp_z$. Based on the two-component density functional theory [11], $\rho(\mathbf{p})$ can be calculated as

$$\rho(\mathbf{p}) = \sum_i n_i^0 \left| \int e^{-i\mathbf{pr}} \psi_{+0}(\mathbf{r}) \psi_i(\mathbf{r}) \sqrt{g(\mathbf{r})} d\mathbf{r} \right|^2, \quad (1)$$

where ψ_i is the wave function of single-particle state within the LDA or GGA with i standing for its state label (containing both band index i and crystal momentum $\mathbf{k}_i$), n_i^0 the occupation number of the ith single-particle state ($=1$ for the valence states and $=0$ for the conduction states), ψ_{+0} the wave function of the thermalized positron, and g is the enhancement factor describing the increase of the contact electron density to positron due to the positron-electron correlation and is calculated within the LDA in the present study [11]. We employ the plane-wave basis set with a cutoff kinetic energy of 10.0 a.u. to expand the wave func-

tions of the electrons and positron. The electron-ion and positron-ion interactions are represented by, respectively, the pseudopotential [12,13] and the full potential using the frozen core approximation (details of the method can be found in our previous publication [10]). In this work, $\rho(\mathbf{p})$ is evaluated at a dense momentum mesh containing 119 164 k points in the first Brillouin zone (FBZ), and the electron wave functions are calculated within the LDA [14] first and then within the GGA [15] for comparison (the GGA calculation uses the ultrasoft pseudopotential [16]).

Although the state-of-the-art facilities and the dense k points are employed in this work, the achieved agreement is found to be similar to our previous work [10]. Namely, as observed in the Compton profiles, the calculation overestimates the momentum densities at low momenta but underestimates at high momenta, and, in the present case, the ACAR density at Γ point is overestimated by about 8%. Nevertheless, this discrepancy is not necessarily the intrinsic error of the LDA, because in the pseudopotential scheme it is difficult to estimate accurately the momentum-density contributions of the positron-electron pairs around the core regions.

To perform reliable and stringent tests, we choose a strategy to focus on the 2D-ACAR anisotropies. The anisotropies are defined as the differences between the 2D-ACAR densities and their cylindrical average [10]; because the momentum-density anisotropies caused by the positron-electron annihilations around the core regions are very small [17], the anisotropies can be regarded as fully arising from the positron-valence-electron annihilations, and furthermore, the downside effect of using the pseudo-wave-functions is also suppressed to be negligible.

Figure 1 presents the anisotropies of the experimental and calculational (LDA) 2D ACAR for Si projected along the [001] direction. General features of the experiment, such as the positive (negative) peaks along the [110] ([100]) and equivalent directions, are well reproduced by the calculation, and their physical origin had been attributed to the occupation of single-electron states at the Jones-zone corners [10]. However, the experimental anisotropies are considerably weaker than the calculated ones. This fact is more explicitly exhibited by the anisotropy cross sections shown in Fig. 2. As seen from Fig. 2, the calculation indeed overestimates the anisotropy peaks, although the differences between the experimental and theoretical anisotropies relative to the peak of the total 2D ACAR are small (less than 2.5%). We have investigated various reasons that may result in the discrepancies. For instance, taking into account the temperature effect by replacing the step function (n_i^0) in Eq. (1) by the Fermi-Dirac distribution, the achieved correction is very small. Actually, the discrepancies are very steady; even using the GGA scheme and a very different type of pseudopotential, quite similar results are obtained and the agreement between theory and experiment is improved only marginally (Fig. 2).

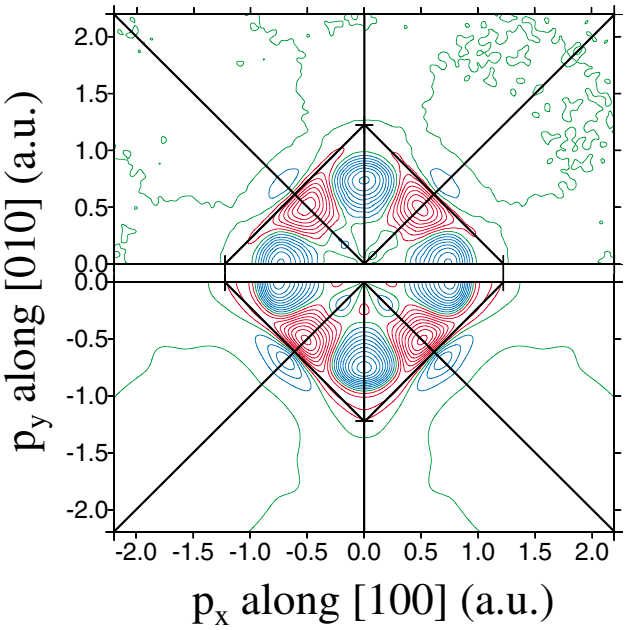

FIG. 1 (color). Experimental (upper) and LDA-calculational (lower) anisotropies of normalized total 2D ACAR projected along the [001] direction in Si. The calculations are convoluted with the experimental resolution of 0.12 a.u. The contour spacing is the same for both plottings (0.005 arbitrary unit). Red, green, and blue lines denote positive, zero, and negative values, respectively. Black lines denote the Jones-zone outline.

Are the discrepancies originated from the LDA or GGA to the exact exchange-correlation potential in the DFT? We investigate this interesting issue by calculating the momentum-density correction due to the electron self-energy using the perturbation method of the quantum field

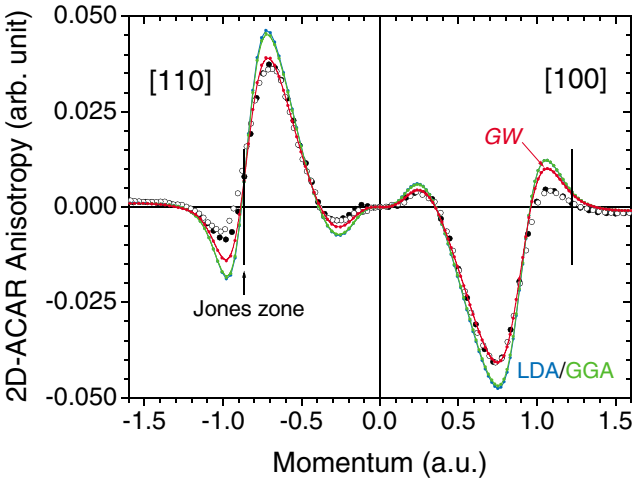

FIG. 2 (color). Cross sections of 2D-ACAR anisotropies ([001] projection) along the [110] and [100] directions in Si. Black solid (open) circles denote the present (previous) experiments. Blue, green, and red colors denote LDA, GGA, and GW calculations, respectively.

theory within the *GW* approximation [13,18–22]. The frequency-dependent, nonlocal exchange-correlation interaction among the LDA single-particle states are introduced through the inverse dielectric matrix, whose plasmon-pole-model form is adopted in the present study [18,19]. The perturbation expansion of the self-energy (Σ) truncated in the first order (i.e., the *GW* approximation) reads (only the ω-dependent part, namely, the correlation energy, is given)

$$\Sigma_i(\omega) = \frac{2\pi}{v} \sum_{\mathbf{GG}'}^{j} \frac{\Omega^2_{\mathbf{GG}'}(\mathbf{q})}{\omega'_{\mathbf{GG}'}(\mathbf{q})} \frac{\rho_{ij}(\mathbf{G})\rho_{ji}(\mathbf{G}')}{|\mathbf{q}+\mathbf{G}||\mathbf{q}+\mathbf{G}'|} \times \left[\frac{n_j^0}{\omega - \varepsilon_j^0 + \omega'_{\mathbf{GG}'}(\mathbf{q}) - i\eta} + \frac{1-n_j^0}{\omega - \varepsilon_j^0 - \omega'_{\mathbf{GG}'}(\mathbf{q}) + i\eta} \right], \quad (2)$$

where v is the volume of the unit cell, μ the chemical potential, ε^0 the LDA eigenenergy, $\mathbf{G}$ ($\mathbf{G}'$) the reciprocal lattice vector, η a positive infinitesimal, $\mathbf{q}$ ($\in$ the FBZ) the reduced momentum transfer of $\mathbf{k}_i - \mathbf{k}_j$, Ω and ω' the plasmon-pole parameters determined by the matrix elements of the inverse dielectric functions directly calculated at two frequencies, and $\rho_{ij}(\mathbf{G}) = \int e^{-i(\mathbf{q}+\mathbf{G})\mathbf{r}} \psi_i^*(\mathbf{r})\psi_j(\mathbf{r}) d\mathbf{r}$.

The real and imaginary parts of the above self-energy [Eq. (2)] give the spectral-density function as

$$A_i(\omega) = \frac{1}{\pi} \frac{|\mathrm{Im}\Sigma_i(\omega)|}{|\omega - \varepsilon_i^0 - \mathrm{Re}\Sigma_i(\omega)|^2 + |\mathrm{Im}\Sigma_i(\omega)|^2}, \quad (3)$$

(only the diagonal part is presented and the nondiagonal parts are omitted), whose frequency integral is the occupation probability of the single-particle state,

$$n_i = \int_{-\infty}^{\mu} A_i(\omega) d\omega. \quad (4)$$

By treating the positron-electron interaction still within the LDA, the momentum density $\rho(\mathbf{p})$ can then be calculated in a fashion analogous to Eq. (1) with the occupation number replaced by the above Eq. (4) [23].

We performed the *GW* calculations for the single-particle states of 32 bands at 2048 k points in the FBZ. For each state, the real and imaginary parts of the self-energy function are directly evaluated at 181 ω points from -3 to 3 a.u. (a small damping of $\eta = 0.01$ a.u. is introduced in numerical calculations to describe the single-particle states coupling with the plasmons [24]). The resulting occupation probabilities are then interpolated to the whole FBZ to calculate $\rho(\mathbf{p})$ at the dense momentum mesh. Special attention is paid to the numerical accuracy; for instance, the sum rule of $\int_{-\infty}^{+\infty} A_i(\omega) d\omega = 1$ is fulfilled with an error less than 0.5%.

As an example, Fig. 3 presents the calculated self-energy functions for the quasiparticle states $\Gamma_{25'}$ (valence) and Γ_{15} (conduction), together with the corresponding spectral-density functions. The quasiparticle's energy is determined by the pole of the Green's function, which is the cross point of $\mathrm{Re}\Sigma(\omega)$ with the straight line of $\omega - \varepsilon^0$. From Fig. 3, it is found that the excitation energy of the $\Gamma_{25'}$ (Γ_{15}) quasiparticle state is shifted by -0.22 (0.38) eV from its LDA eigenenergy, which enlarges the theoretical energy gap at Γ from 2.54 (LDA) to 3.14 eV (*GW*), in good agreement with the experiment (3.4 eV) and other *GW* calculations (3.35 eV) [19].

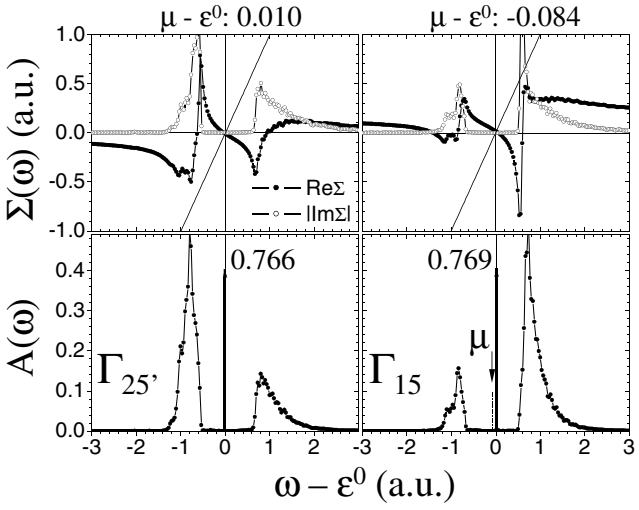

FIG. 3. Self-energy (upper) and spectral-density (lower) functions for the quasiparticle states $\Gamma_{25'}$ and Γ_{15} in Si.

Since no individual electron-hole-pair excitation is taken into account in the present plasmon-pole dielectric function, the single-particle state does not couple with the low-energy elementary excitations, so that $\mathrm{Im}\Sigma$ is zero and the spectral density is a δ function around the quasiparticle energy [its spectral weight is determined by the renormalized factor defined as $Z_F = 1/(1 - \partial\,\mathrm{Re}\Sigma/\partial\omega)$ and the values are marked in Fig. 3]. However, the single-particle states indeed couple with the plasmons, the high-energy density-fluctuation excitations, which results in broad peaks in $\mathrm{Im}\Sigma(\omega)$, and consequently, two sidebands in $A(\omega)$ in addition to the quasiparticle peak. As a result, the occupation probability n after the self-energy correction [Eq. (4)] is less (larger) than one (0) for the valence (conduction) states (Fig. 3). Anyhow, the maximum correction to n^0 (i.e., the deviation from the step function) is found to be less than 0.06, demonstrating the LDA is indeed reasonable enough. As shown in Fig. 4, this self-energy effect decreases (increases) the momentum densities inside (outside) the Jones zone, which can be intuitively viewed as the result of that the fully filled Jones zone is shifted following the momentum of the density fluctuation so that a bunch of electron-hole pairs are collectively created. Especially, this effect is anisotropic (Fig. 4), i.e., the decrease of the momentum-density along the [110]

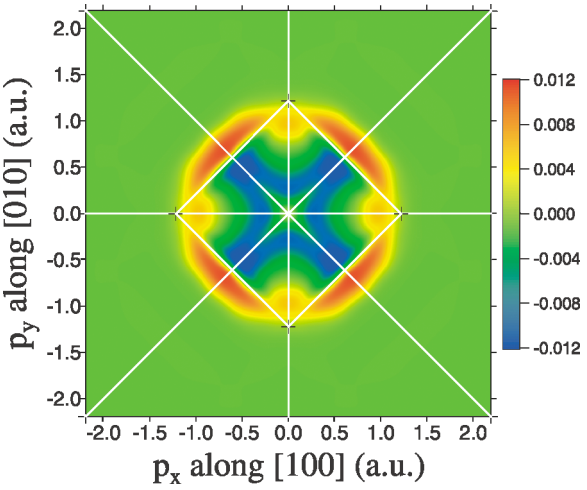

FIG. 4 (color). Self-energy correction, defined as the difference between the normalized *GW* and LDA calculations, to the 2D-ACAR distribution in Si ([001] projection).

direction is larger, which significantly improves the agreement between theory and experiment as shown in Fig. 2.

Good agreement between our *GW* calculation and experiment indicates that the electron-electron correlation has more significant effect than the positron-electron correlation in the ACAR distribution. However, it is noticed that there are still some discrepancies outside the Jones zone (Fig. 2), which may be due to the positron self-energy effect [25] or the conventional position-dependent enhancement factor within the LDA [$g(\mathbf{r})$ in Eq. (1)]. Thus, the positron self-energy correction or a state-dependent enhancement factor [26] is expected to further improve the agreement between theory and experiment and deserves more studies in the future.

In short summary, positron 2D ACAR in Si is employed to test the accuracy and validity of the LDA and *GW* approximation for the momentum-density studies. Carefully conducted experiments and calculations show that there are small but definite discrepancies between the LDA calculation and experiment and that the discrepancies can be decently corrected by the self-energy effect.

We thank our Information Science Group for using the Hitachi SR8000 supercomputer. This work was partly supported by Radioactive Waste Management Funding and Research Center and by Grant-in-Aid for Scientific Research of the Ministry of Education, Culture, Sports, Science, and Technology (Grants No. 12358005, No. 12640334, and No. 13305044).

[1] P. Hohenberg and W. Kohn, Phys. Rev. **136**, B864 (1964); W. Kohn and L. J. Sham, Phys. Rev. **140**, A1133 (1965).
[2] Y. Sakurai *et al.*, Phys. Rev. Lett. **74**, 2252 (1995).
[3] Y. Kubo, J. Phys. Soc. Jpn. **66**, 2236 (1996).
[4] W. Schülke, J. Phys. Soc. Jpn. **68**, 2470 (1999).
[5] C. Sternemann *et al.*, Phys. Rev. B **63**, 094301 (2001).
[6] C. Filippi and D. M. Ceperley, Phys. Rev. B **59**, 7907 (1999).
[7] B. Králik, P. Delaney, and S. G. Louie, Phys. Rev. Lett. **80**, 4253 (1998).
[8] B. Barbiellini, J. Phys. Chem. Solids **61**, 341 (2000).
[9] *Positron Solid-State Physics*, edited by W. Brandt and A. Dupasquier (North-Holland, Amsterdam, 1995).
[10] Z. Tang *et al.*, Phys. Rev. B **57**, 12 219 (1998).
[11] M. J. Puska, A. P. Seitsonen, and R. M. Nieminen, Phys. Rev. B **52**, 10 947 (1995).
[12] N. Troullier and J. L. Martins, Phys. Rev. B **43**, 8861 (1991).
[13] X. Gonze *et al.*, Comput. Mater. Sci. **25**, 478 (2002), and references therein.
[14] D. M. Ceperley and B. J. Alder, Phys. Rev. Lett. **45**, 566 (1980).
[15] J. P. Perdew and Y. Wang, Phys. Rev. B **45**, 13 244 (1992).
[16] G. Kresse and J. Hafner, J. Phys. Condens. Matter **6**, 8245 (1994).
[17] Calculations using an extended full-potential linearized augmented-plane-wave method [Z. Tang *et al.*, Phys. Rev. B **65**, 045108 (2002); M. Hasegawa *et al.*, Appl. Surf. Sci. **194**, 76 (2002)] show that the anisotropies caused by the positron-core-electron annihilations are two orders smaller than those caused by the positron-valence-electron annihilations.
[18] L. Hedin and S. Lundqvist, in *Solid State Physics*, edited by H. Ehrenreich, F. Seitz, and D. Turnbull (Academic, New York, 1969), Vol. 23, p. 1.
[19] M. S. Hybertsen and S. G. Louie, Phys. Rev. B **34**, 5390 (1986).
[20] R. W. Godby and R. J. Needs, Phys. Rev. Lett. **62**, 1169 (1989).
[21] F. Aryasetiawan and O. Gunnarsson, Rep. Prog. Phys. **61**, 237 (1998).
[22] G. Onida, L. Reining, and A. Rubio, Rev. Mod. Phys. **74**, 601 (2002).
[23] Here we still use the DFT-LDA single-particle wave functions because they usually almost overlap with the quasiparticle wave functions; see, for example, Ref. [19].
[24] The small damping broadens the line shape of coupling but has no effect to the occupation probability because of the frequency integral in Eq. (4).
[25] K. Fujiwara, J. Ohyama, and T. Hyodo, J. Phys. Soc. Jpn. **33**, 1047 (1972).
[26] M. Alatalo *et al.*, Phys. Rev. B **54**, 2397 (1996); B. Barbiellini *et al.*, Phys. Rev. B **56**, 7136 (1997).